Structural Optimization 17, 14–24 © Springer-Verlag 1999

Topology optimization using a dual method with discrete variables

M. Beckers

LTAS - Aerospace Structures, University of Liège, 21 rue Ernest Solvay, B-4000 Liège, Belgium

Abstract This paper deals with topology optimization of continuous structures in static linear elasticity. The problem consists in distributing a given amount of material in a specified domain modelled by a fixed finite element mesh in order to minimize the compliance. As the design variables can only take two values indicating the presence or absence of material (1 and 0), this problem is intrinsically discrete. Here, it is solved by a mathematical programming method working in the dual space and specially designed to handle discrete variables. This method is very well-suited to topology optimization, because it is particularly efficient for problems with a large number of variables and a small number of constraints. To ensure the existence of a solution, the perimeter of the solid parts is bounded. A computer program including analysis and optimization has been developed. As it is specialized for regular meshes, the computational time is drastically reduced. Some classical 2-D and new 3-D problems are solved, with up to 30,000 design variables. Extensions to multiple load cases and to gravity loads are also examined.

1 Introduction

Let us consider a domain Ω whose boundary conditions are specified (Fig. 1). The aim of topology optimization is to find the subdomain Ω_m filled with material (or the subdomain Ω_v occupied by the void) in order to satisfy a given criteria, without any *a priori* decision on its connectivity.

The determination of the areas with or without material implies the discretization of the design space. If $\mathbf{x}$ describes the spatial position of a point of Ω, the function $\mu(\mathbf{x})$ indicates the presence or the absence of material in the following way:

- $\mu(\mathbf{x}) = 1$ corresponds to material ($\mathbf{x} \in \Omega_m$),
- $\mu(\mathbf{x}) = 0$ corresponds to void ($\mathbf{x} \in \Omega_v$).

Every integral on the volume of material Ω_m of any function $g(\mathbf{x})$ can be written as an integral on the total volume Ω by multiplying $\mathrm{d}\Omega$ by $\mu(\mathbf{x})$

$$\int_{\Omega_m} g(\mathbf{x})\,\mathrm{d}\Omega = \int_{\Omega} g(\mathbf{x})\mu(\mathbf{x})\,\mathrm{d}\Omega\,. \tag{1}$$

The material is assumed to be isotropic and homogeneous. In linear elasticity and for a single load case, the standard formulation consists of maximizing the global stiffness of the

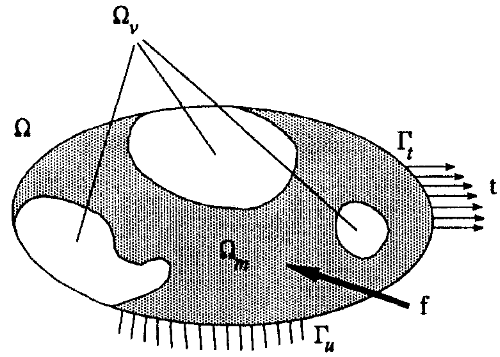

Fig. 1. Design domain (after Bendsøe 1995)

structure, that is equivalent to minimize the compliance, i.e. the work of the external loads. A bound on the volume is a natural cost function. The compliance is written

$$\ell(\mathbf{u}) = \int_{\Omega_m} \mathbf{f}^T\mathbf{u}\,\mathrm{d}\Omega + \int_{\Gamma_t} \mathbf{t}^T\mathbf{u}\,\mathrm{d}\Gamma_t =$$

$$\int_{\Omega} \mathbf{f}^T\mathbf{u}\mu(\mathbf{x})\,\mathrm{d}\Omega + \int_{\Gamma_t} \mathbf{t}^T\mathbf{u}\,\mathrm{d}\Gamma_t\,, \tag{2}$$

where $\mathbf{f}$ is the vector of the body forces, $\mathbf{u}$ is the vector of the displacements that must satisfy equilibrium, compatibility and constitutive equations, $\mathbf{t}$ is the vector of the boundary tractions and Γ_t is the part of the boundary where they are imposed. Here, we consider that the boundary conditions imposed on the displacements (boundary Γ_u) are homogeneous.

The volume is given by

$$V = \int_{\Omega_m} \mathrm{d}\Omega = \int_{\Omega} \mu(\mathbf{x})\,\mathrm{d}\Omega\,. \tag{3}$$

The problem is written as

$$\left\{\begin{array}{l} \displaystyle\min_{\mu(\mathbf{x})\in\{0,1\}} \quad \ell(\mathbf{u}) \\ \text{with} \left\{\begin{array}{l} \displaystyle\int_{\Omega} \mu(\mathbf{x})\,\mathrm{d}\Omega \leq V^{\max} \\ \mathbf{u} \text{ solution of the linear elasticity problem} \end{array}\right. \end{array}\right. . \tag{4}$$

In order to solve it numerically, the design domain is discretized by the finite element method. The discretization of

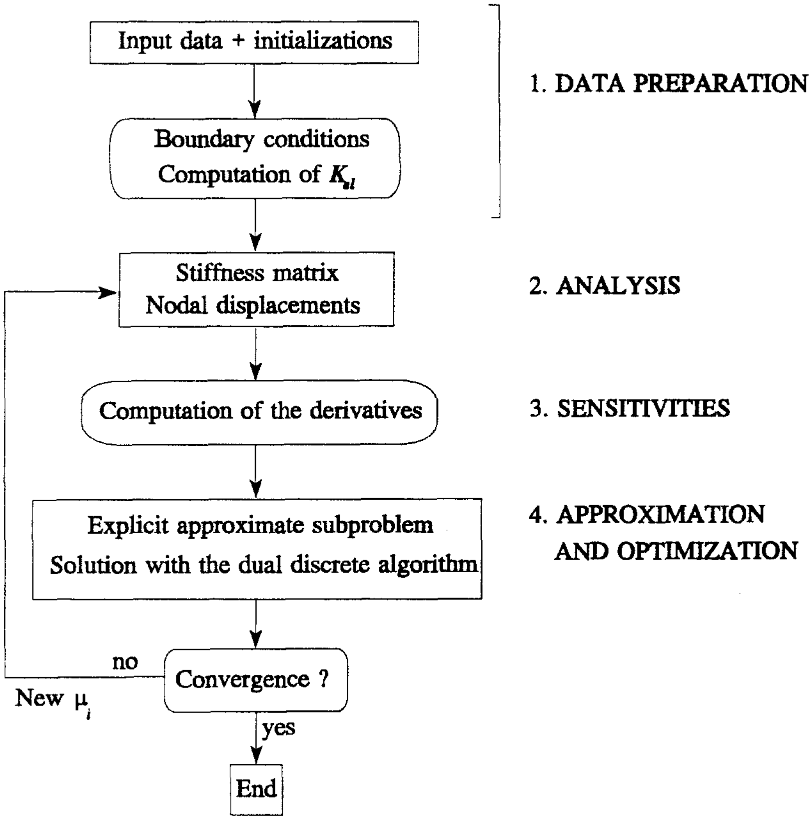

Fig. 2. Flow chart of the program

$\mu(\mathrm{x})$ is naturally performed on the elements; the number n of design variables μ_i, $i = 1, n$ is equal to the number of elements. With cinematically admissible models, the equations of elasticity reduce to the equilibrium equations.

The problem (4) presents two main difficulties.

- It is ill-conditioned and the existence of the solution is not ensured (see e.g. Murat 1977 or Strang and Kohn 1986). Therefore, the computational results are sensitive to the discretization; the more refined the mesh, the more frequent the spatial oscillations of the indicator function. This phenomenon is characterized by alternated void and solid zones, called checkerboards. To avoid this difficulty, a first possibility is to relax the design space by the introduction of perforated microstructures before computing the effective material properties by using homogenization techniques (Bendsøe and Kikuchi 1988). However, the obtained solutions contain some intermediate density areas and are not easy to interpret. A second alternative is to restrict the design space by the imposition of geometrical constraints in order to exclude chattering designs (Buttazzo 1996). Haber *et al.* (1994), as proposed first by Ambrosio and Buttazzo (1993), solve some applications with a bound on the perimeter of the boundary separating material and void, whereas Sigmund (1994) adapts filtering techniques used in digital image processing.

- The design variables μ_i, $i = 1, n$ are binary. Moreover, a high quality solution requirement can only be achieved with many elements, usually several thousands. Generally, the unavailability of discrete algorithms dealing with such a large number of variables requires to approximate the binary problem by a continuous one, either by considering continuous μ_i, $i = 1, n$ and by penalizing values between 0 and 1 (Bendsøe 1989) or by relaxing the design space with the introduction of porous materials.

2 New approach

Here, we propose to solve directly the binary problem (4) by a discrete mathematical programming method working in the dual space, based on the algorithms of Schmit and Fleury (1980) and of Sepúlveda and Cassis (1986). A detailed description of this method and of its application field is given by Beckers (1997). This approach is able to overcome the two difficulties above, because it can handle efficiently a large number of binary variables and because the addition of an upper bound constraint on the perimeter guarantees that the design problem is well-posed. A variant that uses the filter method has also been studied; it has also been combined with the perimeter method. The problem is written

$$\left\{\begin{array}{l}\text{minimization of the compliance}\\ \text{with}\left\{\begin{array}{l}\text{bound on the volume}\\ \text{bound on the perimeter}\\ \text{large number of 0-1 variables}\end{array}\right.\end{array}\right. \tag{5}$$

The equilibrium equations are taken into account when computing the displacements. The dual approach is very well-suited to topology optimization because of the particular

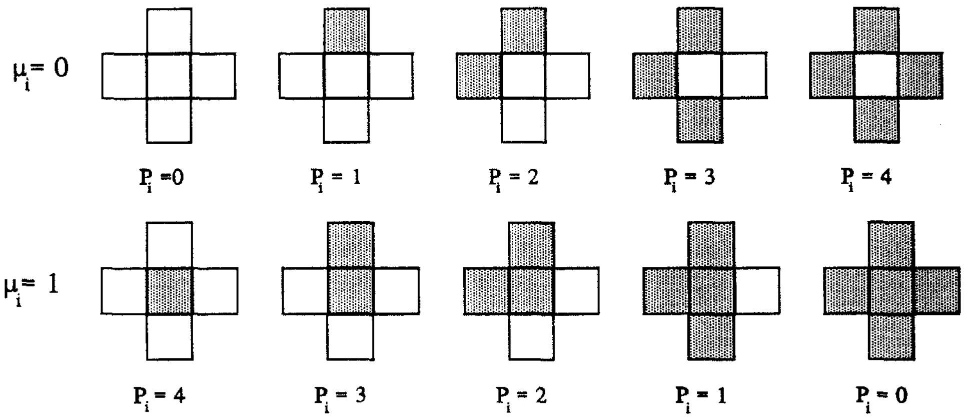

Fig. 3. Possible values of the perimeter of the central element

form of the problem - for a single load case, one or two constraints and a very large number of variables - which induces the consequence that the dual space is only one or two-dimensional.

The compliance cannot be expressed explicitly in terms of the design variables. Therefore, it is necessary to use approximation schemes in order to avoid performing a prohibitive number of analyses during the optimization. Therefore, the process becomes iterative, each loop including the structural and sensitivity (see Section 2.4) analyses, the generation of an explicit subproblem and its solution with the discrete dual algorithm. According to Fleury (1993), it is very advantageous to resort to convex and separable approximation schemes. The convexity ensures equivalence between primal and dual solutions, and the separability leads to simple primal-dual relations. The initial problem is then replaced by a sequence of binary explicit, "convex" and separable subproblems. As a discrete problem is not convex because the primal space is composed of a disjoint set of points, we put "convex" in quotation marks to describe a problem that would be convex if the design variables were continuous, for example the minimization of a convex function under a convex set of constraints but with discrete variables.

2.1 Flow chart

The domain is discretized in n finite elements built on regular grids: rectangular 4-node elements for 2-D applications and parallelepipedic 8-node elements for 3-D applications. This choice is motivated by the high cost of 8-node 2-D elements or 20-node 3-D elements for fine meshes. Moreover, the quality of the finite element mesh has been *a posteriori* controlled for some applications by means of an error estimation (Dufeu 1997). A specific program combining analysis and optimization has been developed, divided in four main steps (Fig. 2). It is especially well-suited to rectangular or parallelepipedic meshes corresponding to the majority of topology examples available in the literature. The procedure allows one to drastically reduce the computation time. It avoids a lot of calculations and of storage. For example, only one elementary stiffness matrix $\mathbf{K}_{e\ell}$ is evaluated and stored. A simple multiplication by μ_i leads to all the others [see (8)].

For reasons explained in Section 3.1, the loop is in practice executed at least 50 times. Since the sensitivity analysis can be performed by simple algebraic formulae and because the optimization problem is very small (two variables), more than 95% of the CPU time is spent on the factorization of the global stiffness matrix, that is performed by a skyline method, particularly efficient for long thin 2-D structures. So, problems with a very high number of variables can be solved.

2.2 Discretization

A binary design variable μ_i is associated with each element i. It indicates the presence of material. For plane stress analysis, Hooke's matrix is

$$\mathbf{H} = \frac{E}{(1-\nu^2)} \begin{pmatrix} 1 & \nu & 0 \\ \nu & 1 & 0 \\ 0 & 0 & \frac{(1-\nu)}{2} \end{pmatrix}, \tag{6}$$

where E is Young's modulus and ν Poisson's ratio. The nodal displacements $\mathbf{q}$ are obtained by solving the equilibrium equations

$$\mathbf{q} = \mathbf{K}^{-1}\mathbf{g}, \tag{7}$$

where $\mathbf{g}$ is the external nodal loads vector. The field of displacements $\mathbf{u}$ is expressed in terms of the nodal values $\mathbf{q}$. The global stiffness matrix $\mathbf{K}$ is assembled from the elementary stiffness matrices $\mathbf{K}_i$ defined as

$$\mathbf{K}_i = \int_{\nu_i} \mathbf{B}_i^T \mathbf{H} \mathbf{B}_i \mu_i \, \mathrm{d}v_i = \mu_i \mathbf{K}_{e\ell}, \tag{8}$$

where $\mathbf{B}_i$ is the strain-displacement matrix and ν_i is the volume of one element. Equation (8) shows that it is sufficient to calculate only one stiffness matrix $\mathbf{K}_{e\ell}$, and then, when assembling, to multiply it by the indicator variable. After obtaining the nodal displacements $\mathbf{q}$ by (7), the compliance is computed by

$$C = \mathbf{q}^T \mathbf{g}. \tag{9}$$

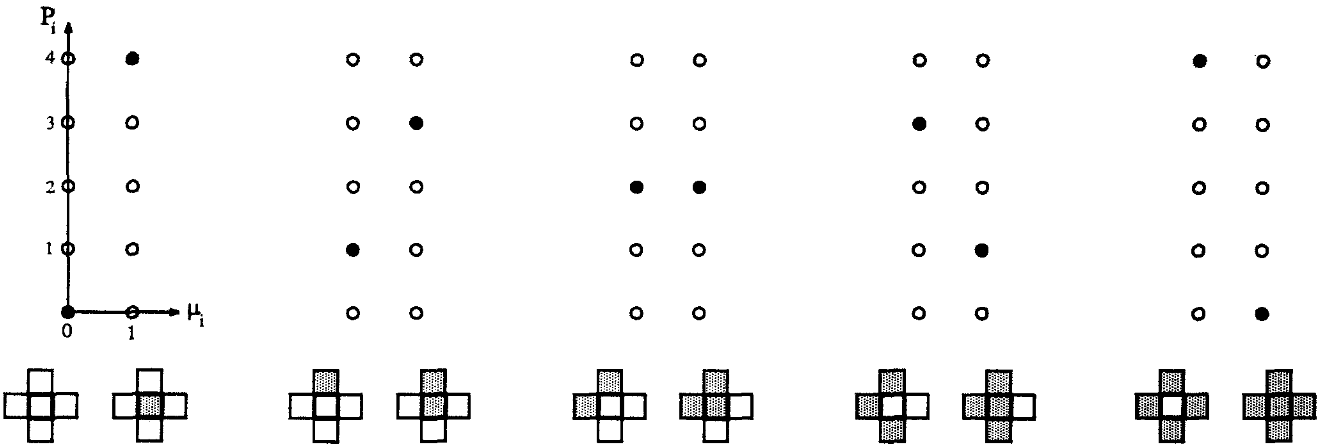

Fig. 4. Evolution of the perimeter for all possible combinations of μ_j and when μ_i changes state

At the equilibrium, it is twice the deformation energy. The problem to be solved is

$$\begin{cases} \min\limits_{\mu} \ \mathbf{q}^T \mathbf{g} \\ \text{with} \begin{cases} \sum\limits_{i=1}^{n} \mu_i v_i \leq V^{\max} \\ \text{perimeter} \ \leq P^{\max} \\ \mu \in \{0,1\}\,,\ i = 1, n \end{cases} \end{cases} \tag{10}$$

It involves a large number n of binary variables but only two constraints. To avoid the treatment of singularities during the analysis stages, the minimum value of the indicator function is chosen as a small but nonzero value: 0.0001 in all the applications presented.

2.3 Perimeter and filter

The perimeter method introduces a global constraint on the structure which acts only on the void-material interfaces. It is a simple geometrical entity, easy to calculate. For two-dimensional structures, the perimeter is the length of the void-solid boundaries. It is computed by adding, for all the interfaces k between two elements i and j, the modulus of the difference between the two indicator variables multiplied by the interface length ℓ_k,

$$P = \sum_{k=1}^{K} \ell_k |\mu_i - \mu_j| \,. \tag{11}$$

For a border, the same formula is used, where the missing neighbour μ_j is replaced by 0, except if the boundary is an axis of symmetry. In this case, μ_j is set to the value μ_i of the other element, in order to work always on the perimeter of the whole structure. If the design variables are not binary, (11) is still applied but the result is no longer a true perimeter.

The function (11) is explicit, but it cannot be used in this form for the optimization, because an efficient solution with a dual method requires separable functions. Then, it is necessary to build a separable approximation of the perimeter, by making the assumption that when the indicator function of one element is modified, the neighbours remain unchanged. Let us consider the perimeter P_i of an element i. To simplify the notations, the elements are assumed to be square and of unit length; P_i is a combinatorial function that can take on 10 different values depending on the state (void or solid) of the four neighbours (Fig. 3). Figure 4 shows the five variations of P_i that are taken into account when μ_i becomes void or solid and under the hypothesis that the variables μ_j of the neighbours are fixed to binary values. As the couplings between neighbours are neglected, the perimeter approximation is not always precise and it is sometimes difficult to satisfy the perimeter bound. This is not so important, because its main role is to allow a control on the quality of the solution.

In the filter method, a lower bound filter is applied to avoid checkerboards, by modifying heuristically the first-order derivatives of the compliance (see Sigmund 1994). Below a fixed length r structural variations are highly penalized, so the thicknesses of structural members are forced to be larger than $2r$ for all meshes. The solutions do not contain any more thin members.

2.4 Sensitivities and approximation schemes

In structural optimization, the classical approximation schemes are based on first-order developments in Taylor series. At the current point, they need the value of the functions and of their derivatives with respect to all the design variables. The sensitivity analysis is generally very expensive, but here, it is realized by means of simple algebraic formulae. After some developments and without body loads, we obtain for the compliance

$$\frac{\partial C}{\partial \mu_i} = -\mathbf{q}_i^T \mathbf{K}_{e\ell} \mathbf{q}_i \,, \quad i = 1, n \,. \tag{12}$$

The volume is linear, so each of its derivatives is the elementary volume v_i. As the perimeter given by (11) is not differentiable at $\mu_i = \mu_j$, Haber *et al.* (1994) propose to modify slightly this formula by introducing a positive real ξ close to zero,

$$P = \sum_{k=1}^{K} \ell_k \left(\sqrt{(\mu_i - \mu_j)^2 + \xi} - \xi \right) \,. \tag{13}$$

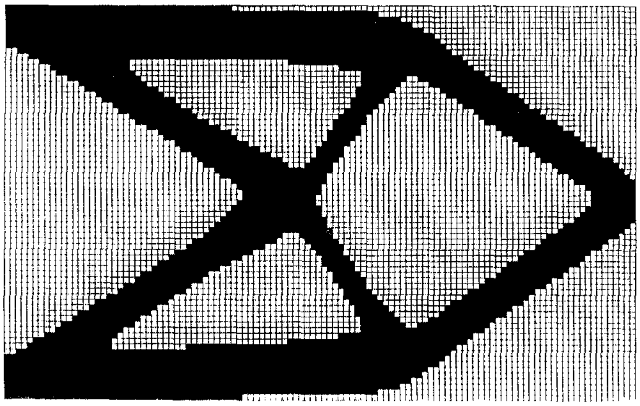

Fig. 5. Michell truss, clamped left side, load at the middle of the right side, 8064 elements; volume of material = 37.5%; bounded perimeter

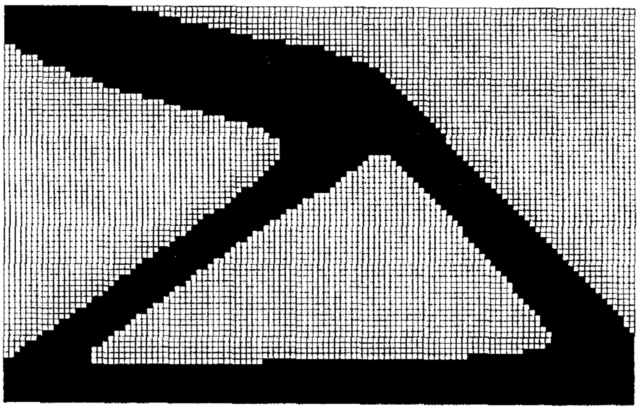

Fig. 6. Michell truss, clamped left side, load at the bottom of the right side, 8208 elements; volume of material = 37.5%; bounded perimeter

As $\partial\mu_j/\partial\mu_i = 0$ if $j \neq i$, only the four interfaces of an element i contribute to the derivative of the perimeter with respect to this variable,

$$\frac{\partial P}{\partial \mu_i} = \sum_{k=1}^{4} \ell_k \frac{\mu_i - \mu_j}{\sqrt{(\mu_i - \mu_j)^2 + \xi^2}} . \tag{14}$$

However, the quantity $|\mu_i - \mu_j|$ is here 0 or 1 because the design variables are binary. As ξ is chosen very small beside the unity, the derivative can be written

$$\frac{\partial P}{\partial \mu_i} = \sum_{k=1}^{4} \begin{cases} +\ell_k & \text{if} \quad \mu_i > \mu_j \\ -\ell_k & \text{if} \quad \mu_i < \mu_j \\ 0 & \text{if} \quad \mu_i = \mu_j \end{cases} . \tag{15}$$

To produce a sequence of good quality approximate subproblems, it is necessary to select an appropriate scheme for each of the three functions. The compliance has a behaviour similar to a displacement. As all its derivatives are negative, it is equivalent to build an explicit approximation by a reciprocal scheme or by the convex linearization scheme (Fleury and Braibant 1986). The volume is linearized. For the perimeter, the choice of a separable approximation is more delicate. If the neighbours of an element remain unchanged, the contribution of one variable to the perimeter is linear; so we choose such an approximation. Two kinds of linear approximation are considered: a local one and a middle range one (based on the value of the perimeter at two points) (see Beckers 1997).

2.5 Solution of the dual problem

Expressed in terms of the Lagrangian multipliers associated with the constraints, the dual problem is continuous and quasi-unconstrained, but not everywhere differentiable. The dual function is a piecewise linear function. Its geometrical representation is a convex polyhedron. It is maximized with a method based on steepest ascent subgradients. The main objection that can be raised to the dual method is the existence of a duality gap, due to the nonconvexity of the primal problem caused by the discrete nature of the design variables. However, this gap is proved to be small if the number of variables (equal here to the number of finite elements) is high and if the number of constraints (2 for a single load case) is low (Bertsekas 1982). As the number of elements has to be important to obtain realistic solutions, the topology optimization problem fulfils both conditions. Moreover, a maximum bound on the duality gap can be calculated and was always negligible in the tested applications.

3 Applications

3.1 Move limit

Since local approximations are precise only in the vicinity of the approximation point, it is necessary to use move limits to maintain their quality and avoid convergence towards local optima. The number of reanalyses, *a priori* chosen, is high; usually, 50 to 150 iterations are performed to reach the solution.

Two distinct move limits are proposed. In the first strategy, the variables remain always binary. At the beginning, the bound on the volume is put to 100% of the total volume of the domain. Then, it is gradually decreased until reaching the required value. In the second approach, two intermediate admissible values are considered at the first iteration (for example close to the percentage of imposed volume). During the process, these two values are progressively modified from their initial value and moved slowly towards 0 and 1

3.2 Nondimensional compliance

A nondimensional parameter can be defined to compare the quality of the solutions. For 2-D problems and for a same loading and a same aspect ratio, the optimal topology needs only to be computed for one set of values of Young's modulus E, load modulus $\| \mathbf{g} \|$ and domain thickness T. For any other values of these variables, optimal values of the compliance can be derived by a simple scaling. The nondimensional compliance is defined as

$$C_{\text{ad}} = C \frac{ET}{\| \mathbf{g} \|^2} . \tag{16}$$

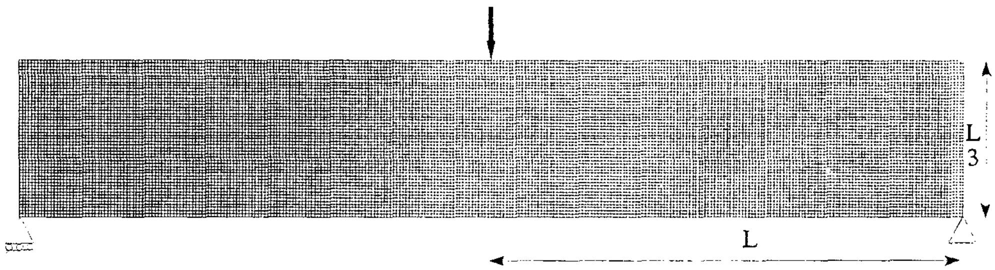

Fig. 7. MBB beam; 15000 elements (only half is studied); 50% of the volume is allowed for material

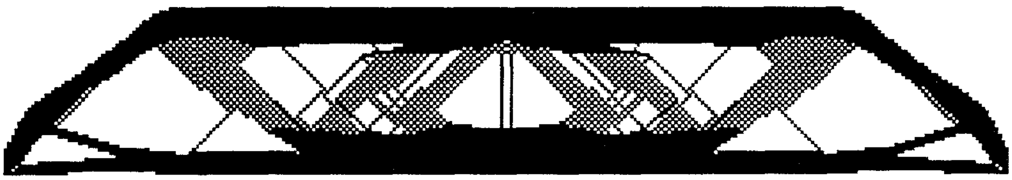

Fig. 8. Typical solution without bounding the perimeter; perimeter = $49L$, $C_{\mathrm{ad}} = 369.7$

Fig. 9. Typical solution with slightly bounded perimeter; perimeter = $31L$, $C_{\mathrm{ad}} = 379.1$

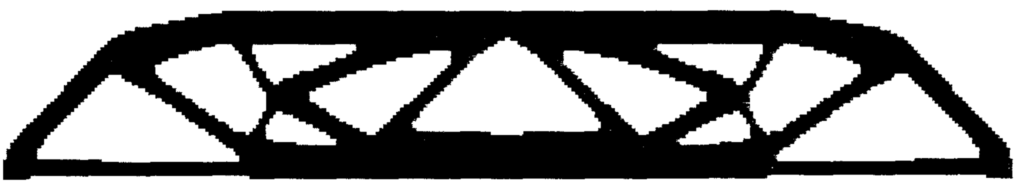

Fig. 10. Typical solution with bounded perimeter; perimeter = $14L$, $C_{\mathrm{ad}} = 376$

For 3-D problems, for the same loading and aspect ratio, the compliance is proportional to $\| \mathrm{g} \|^2$ and inversely proportional to E and to the geometric scale L (that is for example one dimension of the domain). The nondimensional compliance is

$$C_{\mathrm{ad}} = C \frac{EL}{\| \mathrm{g} \|^2} \,. \tag{17}$$

3.3 Two-dimensional solutions

The proposed discrete optimization method has been found to be very efficient in test examples. The results exhibit clean solutions composed only of two states, the absence or presence of material (Figs. 5 and 6). Moreover, the duality gap is negligible. Apart from producing a well-posed problem, the bound on the perimeter allows one to control the number and the dimension of the perforations in the optimal structure (Figs. 8 to 10). For these two applications, we recover the analytical solutions proposed by Rozvany (1998) and a number of numerical results obtained by optimality criteria methods (e.g. Rozvany *et al.* 1995; Haber *et al.* 1996). The nondimensional compliance shows that the quality of the solution is of course increasing when the perimeter is not or slightly bounded, except for Fig. 9 for which the process has been trapped in a local optimum.

Occasionally, some problems of convergence can be observed, due to the presence of many local optima and to the difficulty of establishing a good separable approximation of the perimeter restriction which is highly combinatorial. A variant consisting in adding to the problem with bounded perimeter an image processing filter has been examined. The results show that this modification helps to guide the solution when the bound on the perimeter is small (Fig. 11).

The same problem is solved with three different meshes (Figs. 12 to 14). Here, the final topology is mesh independent. However, the addition of a bound on the perimeter ensures the existence of the solution, but not its uniqueness (Haber *et al.* 1996). All the solutions with high perimeter are eliminated, but a lot of local optima satisfying the perimeter bound can appear.

Fig. 11. Typical solution with filter and bounded perimeter; perimeter $= 11L$, $C_{\rm ad} = 387.5$

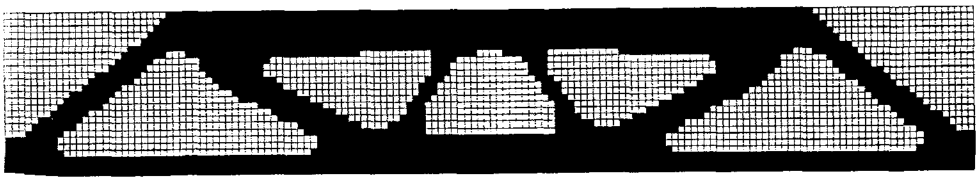

Fig. 12. 25×150 mesh: 3750 elements

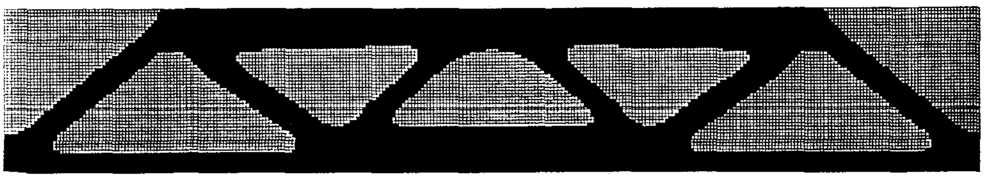

Fig. 13. 50×300 mesh: 15000 elements

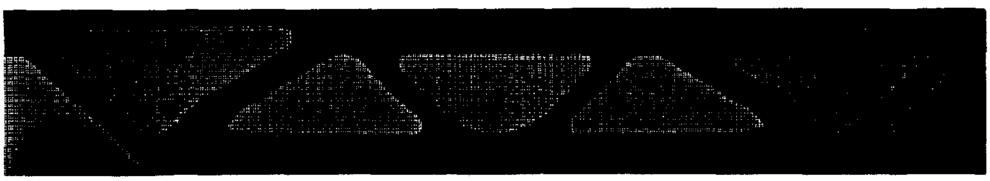

Fig. 14. 100×600 mesh: 60000 elements

3.4 Multiple load cases

In contrast to the methods using optimality criteria, the mathematical programming approach makes the solution of problems with more than one constraint easy. This allows one to take into account the bound on the perimeter, but also to solve problems with multiple load cases. The general statement consists in minimizing the maximum of compliances for each of the p load cases (Achtziger 1993). If the j-th load case gives rise to displacements $\mathbf{u}_j$ and to the compliance $\ell_j(\mathbf{u}_j)$, the problem is written

$$\left\{ \begin{array}{l} \displaystyle\min_{\mu(\mathbf{x})\in\{0,1\}} \max_{j=1,p} \ell_j(\mathbf{u}_j) \\ \text{with} \left\{ \begin{array}{l} \displaystyle\int_\Omega \mu(\mathbf{x})\,\mathrm{d}\Omega \le V^{\max} \\ \text{perimeter} \le P^{\max} \\ \mathbf{u}_j \text{ solution of the } j\text{-th linear elasticity problem,} \\ j = 1,p \end{array} \right. \end{array} \right. \tag{18}$$

By introducing an auxiliary continuous variable, the multiobjective formulation is transformed into a mixed discrete-continuous minimization problem with $2+p$ constraints and the solution algorithm must be modified. As the number of constraints remains low in comparison with the number of variables, the dual approach is still very interesting. Figure 15 (Díaz and Bendsøe 1992) and Fig. 16 show an example with 2 load cases (loads P and loads Q). The solution is very different to the one obtained if the P and Q loads are working simultaneously (Fig. 17).

3.5 Three-dimensional solutions

The developed program can handle a high number of elements in a computationally economical way. Thus it has been extended to perform three-dimensional applications (Beckers 1996). The classical 8-node volume element has been included in the program, and a 3-D perimeter has been defined, equal to the sum of the surfaces between void and solid. When possible, symmetry conditions are imposed. Some examples are illustrated in Figs. 18 to 25. The visualization is obtained with POV-Ray software (1993).

3.6 Problem statement including self-weight loads

To obtain more realistic solutions, we take into account the weight of the structure. As there are body loads, the deriva-

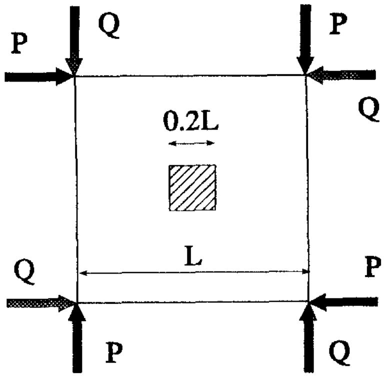

Fig. 15. Boundary conditions

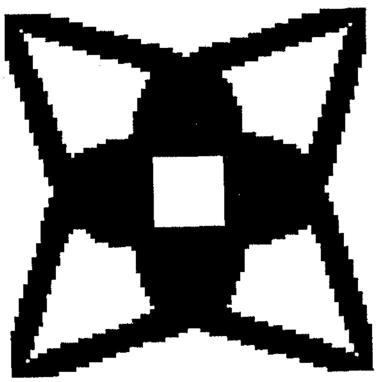

Fig. 16. Solution - multiple load cases

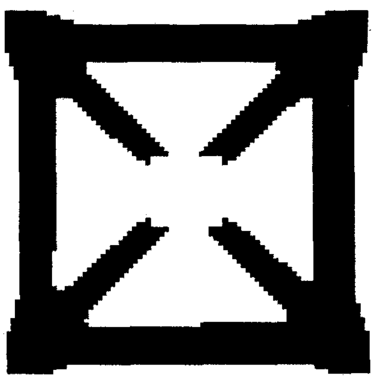

Fig. 17. Solution - single load case

tives (12) of the compliance are modified

$$\frac{\partial C}{\partial \mu_i} = 2\mathbf{q}_i^T \mathbf{g}_{e\ell} - \mathbf{q}_i^T \mathbf{K}_{e\ell} \mathbf{q}_i \,, \quad i = 1, n \,, \tag{19}$$

where $\mathbf{g}_{e\ell}$ is the weight of a solid element. The convex linearization scheme is used to obtain an explicit and convex approximation. An example is presented (Fig. 26), where the total external load equals more or less the weight of the bridge. The optimal structure looks like a two-arch bridge. With the introduction of weight, it is more difficult to obtain the result: between two iterations, it can occur that a lot of void elements switch with solid ones. To stabilize the convergence, it is important to prevent these variations. One way is to add to the objective function a term that penalizes the change of elements state. Another way is to impose a small maximum bound on the perimeter or a filter, which produces

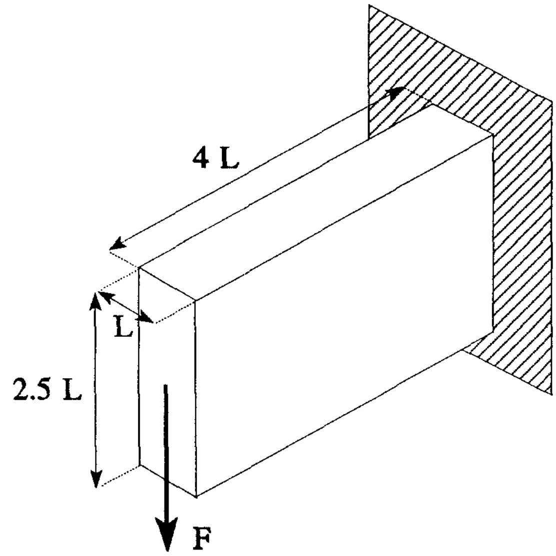

Fig. 18. 3-D Michell truss

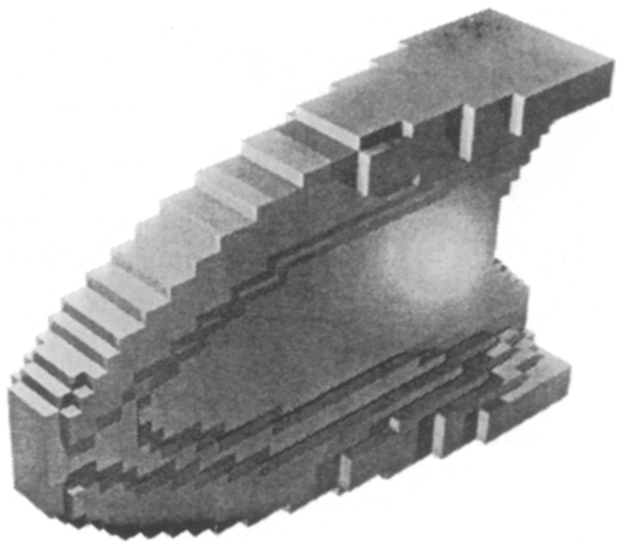

Fig. 19. Bounded perimeter; 17280 elements

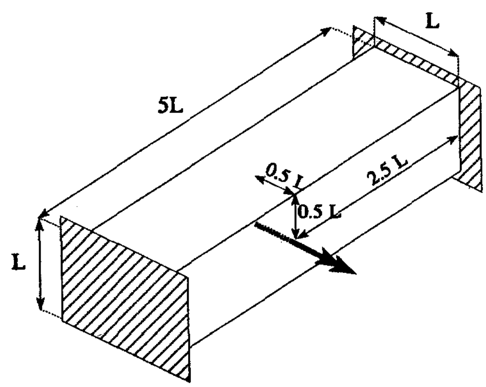

Fig. 20. Embedded beam in torsion

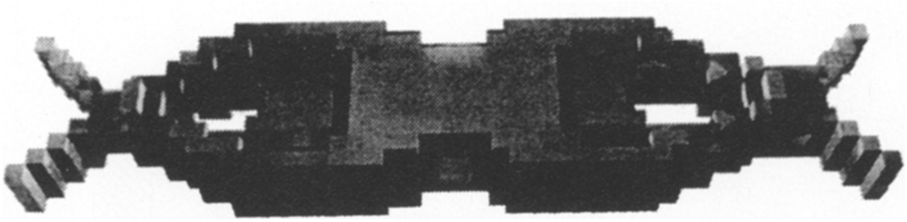

Fig. 21. Bounded perimeter; 5000 elements

a merge of material and so helps to prevent oscillations.

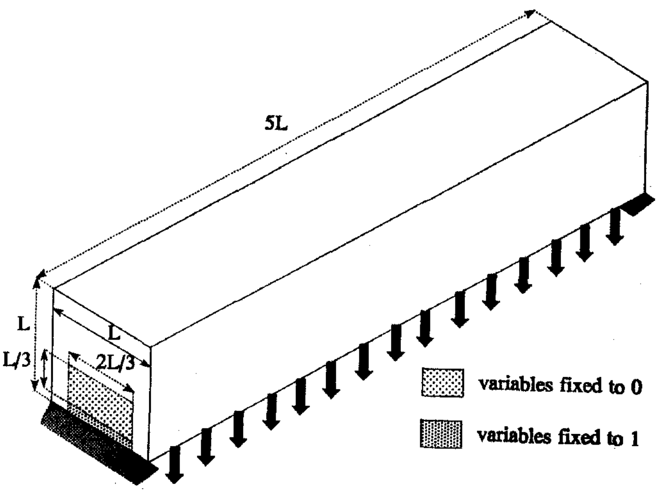

Fig. 22. Bridge

4 Conclusions

The main advantage of the proposed method is its ability to directly solve the problem with 0-1 variables. Therefore, it produces realistic solutions composed only of two states, the absence or presence of material, particularly interesting in 3-D applications. The perimeter bound leads to a well-posed problem and provides a good control of the number and the sizes of perforations in the optimal structure. Moreover, it is a global and easy to calculate constraint. The use of a filter, although rather expensive, helps sometimes to overcome the problems of convergence. Some applications with a large number of elements are solved; the duality gap is always negligible: a maximum bound has been computed and is about 10^{-5} percent of the objective function. With an HP PA 8000 workstation, only 6 minutes of CPU time are needed to obtain the topology of the MBB beam with 7500 variables (Figs. 8 to 11). Less than one hour is sufficient for the same example with 30000 elements (Fig. 14) and for the 3-D Michell truss of Fig. 19.

Acknowledgement

The author wishes to acknowledge the FRIA organization for its supporting grant.

References

Achtziger, W. 1993: Minimax compliance truss topology subject to multiple loadings. In: Bendsøe, M.P.; Mota Soares, C.A. (eds.) *Topology design of structures*, pp. 43-54. Dordrecht: Kluwer

Ambrosio, L.; Buttazzo, G. 1993: An optimal design problem with perimeter penalization. *Calculus of Variations and Partial Differential Equations* 1, 55-69

Beckers, M. 1996: Optimisation topologique de structures tridimensionnelles en variables discrètes. *Rapport OF-44*, L.T.A.S., University of Liège, 1-25

Beckers, M. 1997: *Optimisation de structures en variables discrètes.* Ph.D. Thesis. Collection des publications de la Faculté des Sciences appliquées no. 181, University of Liège

Bendsøe, M.P. 1989: Optimal shape design as a material distribution problem. *Struct. Optim.* 1, 193-202

Bendsøe, M.P. 1995: *Optimization of structural topology, shape and material.* Berlin, Heidelberg, New York: Springer

Bendsøe, M.P.; Kikuchi, N. 1988: Generating optimal topologies in structural design using a homogenization method. *Comp. Meth. Appl. Mech. Engrg.* **71**, 197-224

Bertsekas, D.P. 1982: *Constrained optimization and Lagrange multiplier methods.* New York: Academic Press

Buttazzo, G. 1996: Shape optimization for Dirichlet problems. *Lecture Notes of the Intensive School on Optimal Design Theory and Applications* (held at the University of Pavia, Italy)

Díaz, A.R.; Bendsøe, M.P. 1992: Shape optimization of structures for multiple loading conditions using a homogenization method. *Struct. Optim.* **4**, 17-22

Dufeu, E. 1997: *Calcul d'erreur et adaptation de maillages en 3 dimensions.* Ph.D. Thesis. Collection des publications de la Faculté des Sciences appliqués no. 174, University of Liège

Fleury, C. 1993: Mathematical programming methods for constrained optimization: dual methods and recent developments in structural optimization methods. In: Kamat, M.P. (ed.) *Structural optimization: status and promise*, pp. 123-150, 183-208. AIAA Publication, Progress in Astronautics and Aeronautics **150**

Fleury, C.; Braibant, V. 1986: Structural optimization: a new dual method using mixed variables. *Int. J. Numer. Meth. Engrg.* **23**, 409-428

Haber, R.B.; Jog, C.S.; Bendsøe, M.P. 1994: Variable-topology shape optimization with a control on perimeter. In: Gilmore, B.J.; Hoeltzel, D.A.; Dutta, D.; Eschenauer, H.A. (eds.) *Advances in design automation*, pp. 261-272. Washington D.C.: AIAA

Haber, R.B.; Jog, C.S.; Bendsøe, M.P. 1996: A new approach to variable-topology shape design using a constraint on perimeter. *Struct. Optim.* **11**, 1-12

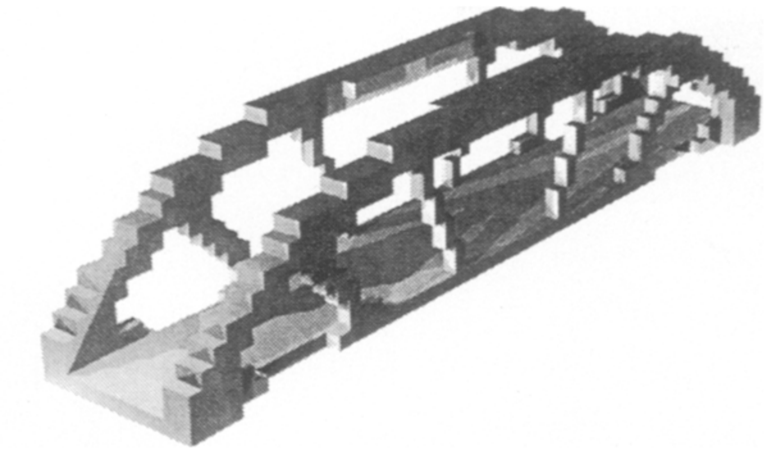

Fig. 23. Bounded perimeter and filter; 8640 elements

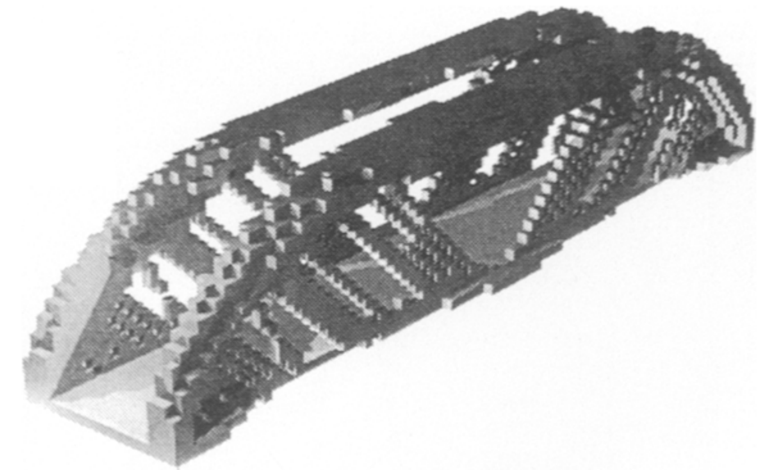

Fig. 24. No bound on the perimeter or filter; 29160 elements

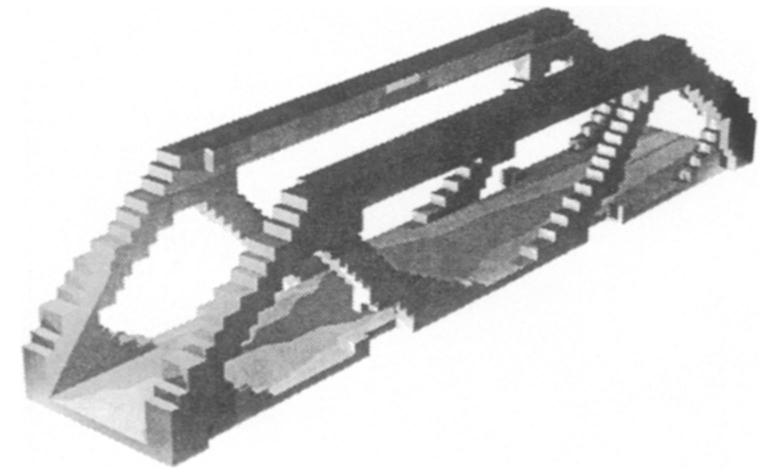

Fig. 25. Bound on the perimeter and filter; 29160 elements

POV-Ray 1993: *Persistence of vision ray tracer, version 2.0, user's documentation.* Copyright POV-Ray Team

Rozvany, G.I.N. 1998: Exact analytical solutions for some popular benchmark problems in topology optimization. *Struct. Optim.* **15**, 42-48

Rozvany, G.I.N.; Bendsøe, M.P.; Kirsch, U. 1995: Layout optimization of structures. *Appl. Mech. Rev.* **48**, 41-119

Schmit, L.A.; Fleury, C. 1980: Discrete-continuous variable structural synthesis using dual methods. *AIAA J.* **18**, 1515-1524

Sepúlveda, A.E.; Cassis, J.H. 1986: An efficient algorithm for the

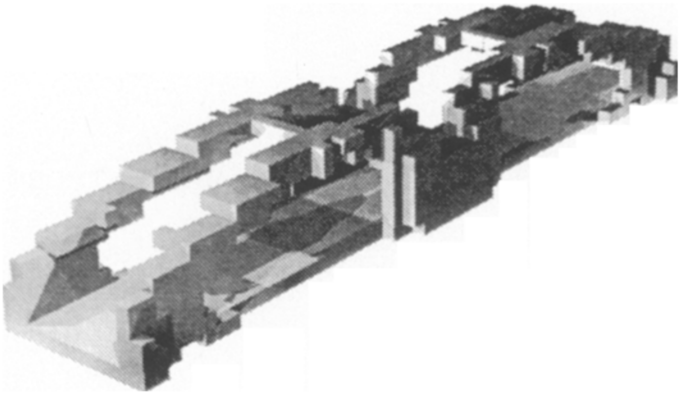

Fig. 26. Solution with gravity load; 8640 elements

optimum design of trusses with discrete variables. *Int. J. Numer. Meth. Engrg.* **23**, 1111-1130

Sigmund, O. 1994: Design of material structures using topology optimization. *DCAMM Special Report No. S69*, Technical University of Denmark

Strang, G.; Kohn, R.V. 1986: Optimal design in elasticity and plasticity. *Int. J. Numer. Meth. Engrg.* **22**, 183-188

Received June 28, 1998
Revised manuscript received November 15, 1998